

Growth rate distribution of NH_4Cl dendrite and its scaling structure

Hiroshi Miki and Haruo Honjo

Department of Applied Science for Electronics and Materials, Interdisciplinary Graduate School of Engineering Sciences, Kyushu University, 6-1 Kasuga-Koen, Fukuoka 816-8580, Japan

(Received 28 February 2012; revised manuscript received 26 October 2012; published 13 December 2012)

Scaling structure of the growth rate distribution on the interface of a dendritic pattern is investigated. The distribution is evaluated for an NH_4Cl quasi-two-dimensional crystal by numerically solving the Laplace equation with the boundary condition taking account of the surface tension effect. It is found that the distribution has multifractality and the surface tension effect is almost ineffective in the unscreened large growth region. The values of the minimum singular exponent and the fractal dimension are smaller than those for the diffusion-limited aggregation pattern. The Makarov's theorem, the information dimension equals one, and the Turkevich-Scher conjecture between the fractal dimension and the minimum singularity exponent hold.

DOI: [10.1103/PhysRevE.86.061603](https://doi.org/10.1103/PhysRevE.86.061603)

PACS number(s): 68.70.+w, 05.45.Df, 89.75.Kd

I. INTRODUCTION

The dendritic pattern is observed in various systems, such as crystallization [1] and electrodeposition [2,3]. It has been one of the most typical and ubiquitous in nonlinear and nonequilibrium physics. A dendritic pattern has a stem with the tip growing stably and steadily, without splitting. Countless sidebranches grow behind the tip due to noise [4] and instability of a flat interface [5]. These sidebranches compete with the ones around them. A longer sidebranch screens off growth of the shorter ones around it. The competition repeats on various length scales, complicated and hierarchical structures are formed [6], and the pattern becomes fractal as a whole.

The growth process of a dendritic pattern is mainly dominated by diffusion and anisotropy. The dendritic pattern is often compared with the diffusion-limited aggregation (DLA) [7] pattern, for which the growth process is also dominated by diffusion. However, there is no anisotropy in the DLA growth process and the DLA pattern is formed through repeat of tip-splitting. It has been reported for an electrodeposition experiment that a transition between dendritic pattern and DLA pattern is observed as the electrolyte concentration and applied voltage are varied [2,3]. Furthermore, the dendritic pattern can be formed artificially by introducing anisotropy into isotropic viscous fingering [8,9] and, on the other hand, the DLA pattern by removing the anisotropy from an anisotropic crystal growth process [10].

The scaling structure and fractality of dendritic pattern have been interesting and important issues for quantitative characterization. It has been reported that the area fractal dimension D_f of a dendritic pattern with fourfold symmetry is 1.5–1.6 for a noise-reduced DLA simulation on a square lattice [11] and NH_4Br crystal growth [12]. It is clearly less than that of the DLA, $D_f \sim 1.71$. This is attributed to the fact that the tip is stabilized against splitting by anisotropy. Mathematically, the lower bound of the fractal dimension for the DLA on a square lattice is proved to be $3/2$ [13].

To characterize a pattern in more detail, the fractal dimension alone is insufficient. For the DLA, the growth rate distribution on the interface is found to have multifractality in the cases of a simulation [14], a crystallization experiment [15], and a conformal mapping model [16–18]. In the present article, we investigate the scaling structure of the growth

rate distribution, especially compared with that of the DLA. We evaluate the growth rate distribution numerically and implement the similar multifractal analysis for a dendritic pattern formed in NH_4Cl crystallization experiment, where the surface tension is effective within a certain length scale.

II. EXPERIMENT

We use an NH_4Cl solution growth dendritic crystal with well-developed sidebranches. The details of our experiment are described in Ref. [6]: An NH_4Cl aqueous solution saturated at approximately 40°C is sealed, with a nucleation seed left in it, in a Hele-Shaw cell, a narrow space between two glass plates. The thickness of the cell is $100\ \mu\text{m}$. Then, when the temperature is lowered (to approximately 30°C), the solution becomes supersaturated, nucleation takes place from the seed, and a growing crystal is observed. The direction of the tip growth is $\langle 100 \rangle$ in the supersaturated solution and the growing dendritic crystal has fourfold symmetry. Sidebranches grow behind the tip and perpendicularly to the stem, with small sub-sidebranches perpendicular to them. The image of the crystal is obtained by a microscope and a charge-coupled device (CCD) camera, whose resolution is 640×480 pixels. The image is binarized by an image processing. The binarized image of a crystal interface is shown in Fig. 1.

The tip growth velocity v_{tip} is $40\text{--}49\ \mu\text{m/s}$. In this case, sidebranches are well-developed within the shooting window, as shown in Fig. 1. However, since the spacing between them is smaller than the diffusion length, they are still competing each other, not growing independently. The diffusion length near the tip $l_D = 2D/v_{\text{tip}}$, where D is the diffusion constant of NH_4Cl ($2.6 \times 10^3\ \mu\text{m}^2/\text{s}$; Ref. [19]) is $\gtrsim 100\ \mu\text{m}$, and that near a sidebranch is longer than this. Therefore, the growth is regarded as quasi-two-dimensional.

III. GROWTH RATE EVALUATION

In principle, it is a faithful method to the original data to evaluate the growth rate from the growth site area between two successive images, as implemented for a DLA pattern [15]. However, for a dendritic pattern, it is quite difficult to implement with satisfactory precision due to the limitation of the resolution and since the difference of the growth rates

between the fast region (around the tips of the stem and longer sidebranches) and the slow region (deep inside the forest of sidebranches) is much larger than that for the DLA. Therefore, instead, we evaluate the growth rate $p_{\text{gr}}(\mathbf{r}_{\text{int}})$ at a point \mathbf{r}_{int} on the interface by the gradient of the concentration field $\phi(\mathbf{r})$,

$$p_{\text{gr}}(\mathbf{r}_{\text{int}}) \sim |\nabla\phi(\mathbf{r})|, \quad (1)$$

where $\phi(\mathbf{r})$ is assumed to satisfy the Laplace equation, $\nabla^2\phi(\mathbf{r}) = 0$, outside of the pattern. This assumption is valid if the diffusion length is larger than the characteristic length scale of the system, for example, the tip radius of the stem or the average spacing of the sidebranch generation. In this case, the characteristic length scale is of the order of $1 \mu\text{m}$; thus, the condition is satisfied.

The Laplace equation for the concentration field is numerically solved by the relaxation method on a square lattice, whose spacing is set to be the pixel size. The concentration is supersaturated far away from the interface (the saturated concentration at 40°C , $46 \text{ g per } 100 \text{ g water}$) and the Gibbs-Thomson boundary condition is imposed at the interface [20,21],

$$\phi(\mathbf{r}_{\text{int}}) = \phi_0[1 + d(\theta)\kappa(\mathbf{r}_{\text{int}})], \quad (2)$$

$$d(\theta) = d_0[1 - \cos(4\theta)], \quad (3)$$

where ϕ_0 denotes the saturation concentration (at 30°C , $41 \text{ g per } 100 \text{ g water}$), $d(\theta)$ the surface tension coefficient with stiffness and fourfold symmetry taken into account, $d_0 = 2.24 \text{ \AA}$ [22] the capillary length, and $\kappa(\mathbf{r}_{\text{int}})$ the local curvature at \mathbf{r}_{int} , respectively. The growth angle θ is defined as the angle between the growth direction at \mathbf{r}_{int} and that of the stem. The curvature and growth angle are calculated by spline interpolation for the pixel data of the crystal interface.

The range in which the growth rate takes value is vast. In the whole interface, the ratio of the largest growth rate to the smallest is more than 10^{10} . Even within the region around the tip of the stem, the ratio is more than 10^4 .

When the surface tension effect is taken into account, there may be a lattice point where the curvature radius is smaller than the lattice spacing. The curvature may vary abruptly from point to point around such a lattice point. If this situation occurs deep inside the forest of well-developed sidebranches, around their roots, a large growth rate, of the same order as that of the tips of the stem or longer sidebranches, may be generated. This is unnatural since the growth in the region is strongly suppressed. In order to appropriately take account of the surface tension effect and phenomenologically circumvent the above unnatural situation, we consider three cases below: (i) The surface tension is completely neglected. In other words, at the interface we set $\phi(\mathbf{r}_{\text{int}}) = \phi_0$ uniformly. Since the typical length scale of the system is of the same order as the lattice spacing and can be regarded as the length scale within which the surface tension is effective, this setting is reasonable. This case is labeled ‘‘Laplace.’’ In this setting the growth rate distribution is the harmonic measure. (ii) A cutoff κ_c is introduced. If $|\kappa| > \kappa_c$, $|\kappa|$ is replaced with κ_c . Here, we set $\kappa_c = 0.01$ times the reciprocal of the lattice spacing. This case is labeled ‘‘cutoff (1).’’ (iii) The surface tension effect is taken into account only around the tips of the stem and sidebranches

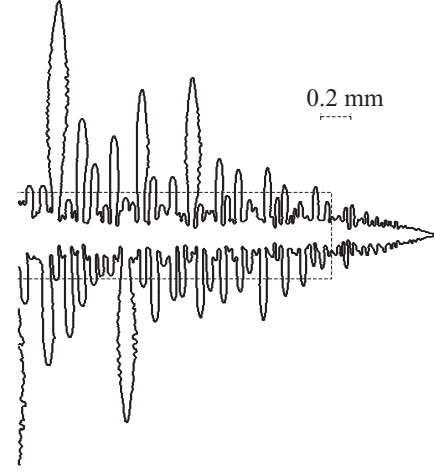


FIG. 1. Image of a dendritic crystal. The resolution is $5.5 \mu\text{m}/\text{pixel}$. Its fractal dimension is 1.54. The region inside the broken line is the cutoff region where the surface tension effect is neglected in our analysis.

and is neglected deep in the sidebranches, in the region shown in Fig. 1. This case is labeled ‘‘cutoff (2).’’ The dependence of the results on how to choose κ_c for the cutoff (1) case and the cutoff region for the cutoff (2) case is very weak as long as κ_c^{-1} is large enough and the cutoff region is wide enough, respectively, to suppress the generation of the unnaturally large growth rate.

IV. MULTIFRACTAL ANALYSIS

Let us consider that the interface of the dendritic crystal is covered by disjoint boxes of size ϵ and let $p_j(\epsilon)$ be the growth rate in the j th box,

$$p_j(\epsilon) = \sum_{\mathbf{r}_{\text{int}} \in j\text{th box}} p_{\text{gr}}(\mathbf{r}_{\text{int}}). \quad (4)$$

The rate $p_j(\epsilon)$ is normalized to be a probability measure, $\sum_j^{N(\epsilon)} p_j(\epsilon) = 1$, where $N(\epsilon)$ is the number of boxes necessary to cover the interface completely. The generalized dimension $D(q)$ is defined as [23]

$$D(q) = \frac{1}{q-1} \lim_{\epsilon \rightarrow 0} \frac{\log Z(\epsilon, q)}{\log \epsilon}, \quad (5)$$

for $q \neq 1$, where $Z(\epsilon, q)$ is the partition function

$$Z(\epsilon, q) = \sum_j^{N(\epsilon)} \{p_j(\epsilon)\}^q. \quad (6)$$

For $q = 1$,

$$D(1) = \lim_{\epsilon \rightarrow 0} \frac{\sum_j^{N(\epsilon)} p_j(\epsilon) \log p_j(\epsilon)}{\log \epsilon}. \quad (7)$$

Practically $D(q)$ is evaluated from the slope of $\log Z(\epsilon, q)$ for $\log \epsilon$ by least squares method.

The singularity exponent $\alpha = \alpha(q)$ and its fractal dimension $f(\alpha) = f(\alpha(q))$ are obtained as functions of q by the Legendre transformation of the generalized dimension

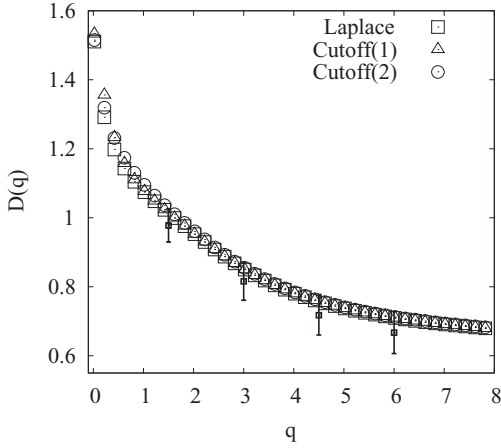


FIG. 2. Generalized dimension $D(q)$, $q > 0$, for the three cases for the pattern shown in Fig. 1. The increment Δq is 0.2. The error bars are obtained over 13 samples for the “Laplace” case.

$D(q)$ [24]:

$$\alpha(q) = \frac{d}{dq} [(q - 1)D(q)], \quad (8)$$

$$f[\alpha(q)] = q\alpha(q) - (q - 1)D(q). \quad (9)$$

However, it is not practical to evaluate α and $f(\alpha)$ from Eqs. (8) and (9), since it may produce relatively large numerical errors. Therefore, instead we adopt a direct evaluation method presented in Ref. [25] described below.

First, let us construct a new probability measure $\mu_j(\epsilon, q)$ with parameter q from $p_j(\epsilon)$ as

$$\mu_j(\epsilon, q) = \frac{\{p_j(\epsilon)\}^q}{\sum_j^{N(\epsilon)} \{p_j(\epsilon)\}^q}. \quad (10)$$

Then, let us define $\zeta(\epsilon, q)$ and $\xi(\epsilon, q)$ as

$$\zeta(\epsilon, q) = \sum_j \mu_j(\epsilon, q) \log[p_j(\epsilon)], \quad (11)$$

$$\xi(\epsilon, q) = \sum_j \mu_j(\epsilon, q) \log[\mu_j(\epsilon, q)]. \quad (12)$$

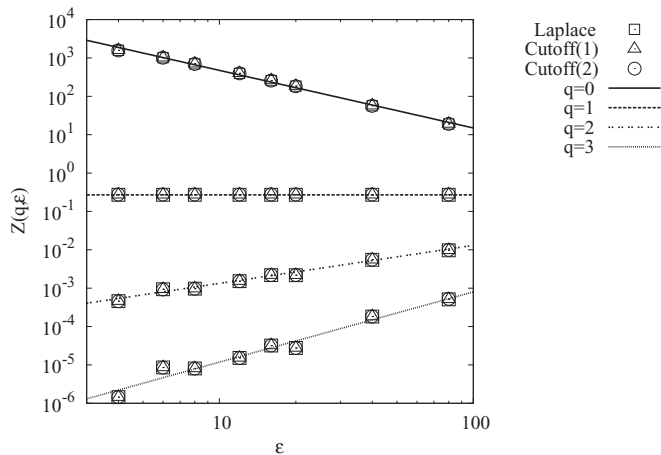


FIG. 3. Log-log plots of $Z(q, \epsilon)$ for the pattern shown in Fig. 1 against the box size ϵ for $q = 0, 1, 2$, and 3 . Note that the slopes mean $(q - 1)D(q)$. For visibility, the measure is not normalized to be a probability [$Z(q = 1, \epsilon)$ is the total sum of the growth rate].

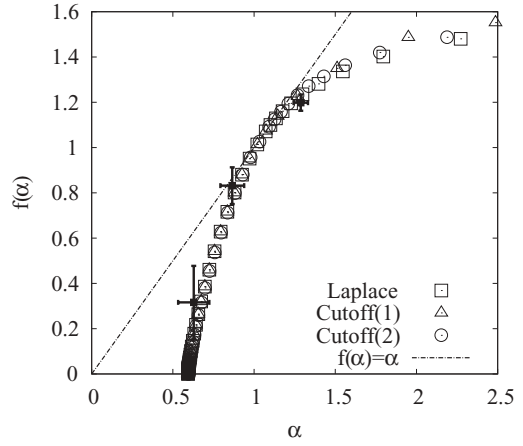


FIG. 4. Results of the multifractal f - α spectrum for the three cases for the pattern shown in Fig. 1. The contact point with the line $f(\alpha) = \alpha$ gives the information dimension $D(1) = \alpha(q = 1) = f[\alpha(q = 1)]$. The increment Δq is 0.1 for $q < 1$ and 0.2 for $q > 1$. The error bars, corresponding to $q = 0.5, 1.5$, and 3 , are obtained over 13 samples for the “Laplace” case.

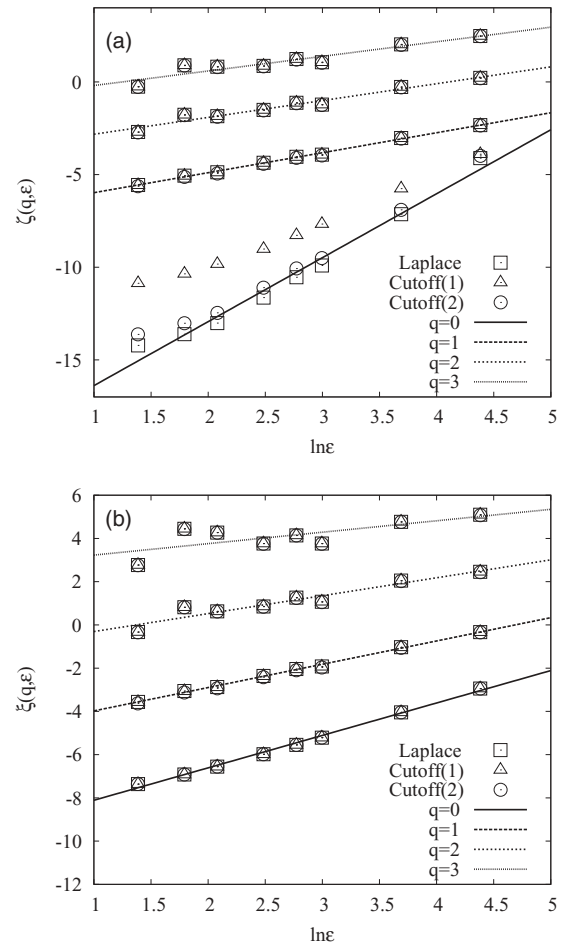


FIG. 5. Fitting of α and f for $q = 0, 1, 2$, and 3 . (a) Plots of $\zeta(q, \epsilon)$ against $\log \epsilon$. (b) Plots of $\xi(q, \epsilon)$. The fitting lines are shown for the “Laplace” case.

TABLE I. List of characteristic scaling exponents. The averages and errors are obtained over 13 samples. Note that D_f is the fractal dimension of the area of the pattern and $D(0)$ is the fractal dimension of the interface, on which the growth rate measure is defined, and that by definition, $\alpha_{\min} = D(q \rightarrow \infty)$. The values for DLA are cited from the results of a conformal mapping model [17,18].

Case	D_f	$D(0)$	$D(1)$	α_{\min}
Laplace	1.55 ± 0.04	1.53 ± 0.02	1.02 ± 0.03	0.56 ± 0.04
Cutoff(1)	1.55 ± 0.04	1.53 ± 0.02	1.03 ± 0.03	0.56 ± 0.04
Cutoff(2)	1.55 ± 0.04	1.53 ± 0.02	1.07 ± 0.03	0.58 ± 0.05
DLA	1.713 ± 0.003	~ 1.71	–	0.665 ± 0.004

From Eqs. (11) and (12), α and $f(\alpha)$ are, as functions of q , given as

$$\alpha(q) = \lim_{\epsilon \rightarrow 0} \frac{\zeta(\epsilon, q)}{\log \epsilon}, \quad (13)$$

$$f(q) = \lim_{\epsilon \rightarrow 0} \frac{\xi(\epsilon, q)}{\log \epsilon}. \quad (14)$$

Practically, they are evaluated from the slopes of $\zeta(\epsilon, q)$ and $\xi(\epsilon, q)$ for $\log \epsilon$, respectively, by the least-squares method. It is easy to show that the definition Eqs. (13) and (14) satisfy the relation Eqs. (8) and (9) by direct calculation.

V. RESULTS AND DISCUSSION

We are interested in the larger growth rate regime, $q \geq 0$. For the pattern of Fig. 1, the results of $D(q)$ for the three cases are shown in Fig. 2. The log-log plots of $Z(q, \epsilon)$ against the box size ϵ and least-squares fitting for several values of q are shown in Fig. 3. The box size is chosen from 4 to 80 pixels, taking the thickness of branches into account. There is a good agreement between the results of the three cases.

The results of the multifractal f - α spectrum for the three cases for the pattern of Fig. 1 in the small α region corresponding to $q \geq 0$ are shown in Fig. 4. These spectra are evaluated by Eqs. (10)–(14) and the plots of $\zeta(q, \epsilon)$ and $\xi(q, \epsilon)$ against $\log \epsilon$ are shown in Fig. 5. There is a good agreement between the results of the three cases, except for $\zeta(q = 0, \epsilon)$. This disagreement is attributed to the surface tension effect, especially the contribution of the growth at points deep inside the forest of sidebranches, with curvature $|\kappa| \sim \kappa_c$. The relatively small difference of $\zeta(q = 0, \epsilon)$ between for the ‘‘Laplace’’ and the ‘‘Cutoff (2)’’ case and the agreement of $\zeta(q, \epsilon)$, $q = 1, 2$, and 3 , for the three cases indicate that the surface tension effect is almost ineffective in the unscreened large growth region. The fact that $D(q)$ and $f(\alpha)$ take continuous values and depend on q or α means that the growth rate distribution has multifractality.

Some characteristic values for the scaling exponents are summarized in Table I, along with those for DLA conformal mapping model [17,18] for comparison. Both the fractal

dimensions of area D_f and perimeter length $D(0)$ are about 1.5, manifestly smaller than those for the DLA. This result agrees with the results of on-lattice simulation [11] and mathematics [13]. The smallest singularity exponent is obtained at the tip of the stem where the growth is most active and it is also smaller than that for the DLA. Furthermore, this agrees with the Turkevich-Scher scaling conjecture $D_f = 1 + \alpha_{\min}$ [26,27], which argues that the fractal dimension depends only on the scaling behavior of the growth of the most active domain. Note that it is clear that the tip of the stem is the most actively growing domain for a dendritic pattern, while it is reported that for the DLA, the most active growth domain is not the outermost tip [18]. The information dimension $D(1)$ is regarded as the fractal dimension of the active zone where the growth is not screened [28]. It is proved by Makarov [29] that exactly $D(1) = 1$ for the harmonic measure. Our results agree with the theorem, remarkably even though the surface tension is taken into account.

VI. CONCLUSION

We evaluated the growth rate distribution of an NH_4Cl dendritic crystal interface by numerically solving the Laplace equation and investigated its scaling property. The effect of the surface tension is taken into account as the Gibbs-Thomson boundary condition with some types of cutoff introduced based on phenomenologically plausible assumptions. We found that in the unscreened large growth rate regime, the distribution has multifractality and the surface tension effect is not essential. The fractal dimension and the value of the smallest singular exponent are smaller than that of the DLA and consistent with the previous results given in theory and simulation. Our results agree with the Makarov’s theorem for the harmonic measure, $D(1) = 1$, and the Turkevich-Scher scaling conjecture, $D_f = 1 + \alpha_{\min}$ in spite of the surface tension effect.

ACKNOWLEDGMENT

This research was supported by the Japan Ministry of Education, Culture, Sports, Science and Technology, Grant-in-Aid for Scientific Research, Grant No. 21540392.

- [1] S. C. Huang and M. E. Glicksman, *Acta Metall.* **29**, 701 (1981); **29**, 717 (1981).
 [2] Y. Sawada, A. Dougherty, and J. P. Gollub, *Phys. Rev. Lett.* **56**, 1260 (1986).

- [3] D. Grier, E. Ben-Jacob, R. Clarke, and L. M. Sander, *Phys. Rev. Lett.* **56**, 1264 (1986).
 [4] A. Dougherty, P. D. Kaplan, and J. P. Gollub, *Phys. Rev. Lett.* **58**, 1652 (1987).

- [5] W. W. Mullins and R. F. Sekerka, *J. Appl. Phys.* **34**, 323 (1963); **35**, 444 (1964).
- [6] K. Kishinawa, H. Honjo, and H. Sakaguchi, *Phys. Rev. E* **77**, 030602 (2008); K. Kishinawa and H. Honjo, *J. Phys. Soc. Jpn.* **94**, 024802 (2010).
- [7] T. A. Witten and L. M. Sander, *Phys. Rev. Lett.* **47**, 1400 (1981); *Phys. Rev. B* **27**, 5686 (1983).
- [8] E. Ben-Jacob, R. Godbey, N. D. Goldenfeld, J. Koplik, H. Levine, T. Mueller, and L. M. Sander, *Phys. Rev. Lett.* **55**, 1315 (1985); E. Ben-Jacob, P. Garik, T. Mueller, and D. Grier, *Phys. Rev. A* **38**, 1370 (1988).
- [9] T. Honda, H. Honjo, and H. Katsuragi, *J. Cryst. Growth* **275**, e225 (2005); *J. Phys. Soc. Jpn.* **75**, 034005 (2006).
- [10] H. Honjo, S. Ohta, and M. Matsushita, *J. Phys. Soc. Jpn.* **55**, 2487 (1987).
- [11] P. Meakin, *Phys. Rev. A* **36**, 332 (1987).
- [12] Y. Couder, F. Argoul, A. Arneodo, J. Maurer, and M. Rabaud, *Phys. Rev. A* **42**, 3499 (1990).
- [13] H. Kesten, *Stochast. Proc. Appl.* **25**, 165 (1987).
- [14] Y. Hayakawa, S. Sato, and M. Matsushita, *Phys. Rev. A* **36**, 1963 (1987).
- [15] S. Ohta and H. Honjo, *Phys. Rev. Lett.* **60**, 611 (1988).
- [16] B. Davidovitch, M. H. Jensen, A. Levermann, J. Mathiesen, and I. Procaccia, *Phys. Rev. Lett.* **87**, 164101 (2001).
- [17] M. H. Jensen, A. Levermann, J. Mathiesen, and I. Procaccia, *Phys. Rev. E* **65**, 046109 (2002).
- [18] M. H. Jensen, J. Mathiesen, and I. Procaccia, *Phys. Rev. E* **67**, 042402 (2003).
- [19] A. Tanaka and M. Sano, *J. Cryst. Growth* **125**, 59 (1992).
- [20] J. S. Langer, *Rev. Mod. Phys.* **52**, 1 (1980).
- [21] J. J. Hoyt, M. Asta, and A. Karma, *Mater. Sci. Eng. R* **41**, 121 (2003).
- [22] A. Dougherty and F. Stinner, arXiv:1206.4030.
- [23] H. G. E. Hentschel and I. Procaccia, *Physica D* **8**, 435 (1983).
- [24] T. C. Halsey, M. H. Jensen, L. P. Kadanoff, I. Procaccia, and B. I. Shraiman, *Phys. Rev. A* **33**, 1141 (1986).
- [25] A. Chhabra and R. V. Jensen, *Phys. Rev. Lett.* **62**, 1327 (1989).
- [26] L. A. Turkevich and H. Scher, *Phys. Rev. Lett.* **55**, 1026 (1985).
- [27] T. C. Halsey, P. Meakin, and I. Procaccia, *Phys. Rev. Lett.* **56**, 854 (1986).
- [28] A. Coniglio and H. E. Stanley, *Phys. Rev. Lett.* **52**, 1068 (1984).
- [29] N. G. Makarov, *Proc. Lond. Math. Sci.* **51**, 369 (1985).